A Wideband Double-Balanced Multiplier Integrated Circular-Polarization Switchable Microstrip Antenna with Parasitic Elements

Tatsuki KAYASHIMA[†a)], ***Student member***, **Eisuke NISHIYAMA**[†b)] ***and*** **Ichihiko TOYODA**[†c)], ***Senior members***

SUMMARY This paper presents a new wideband circular-polarization (CP) switchable microstrip antenna. The novel concept of the wideband operation is a combination of a double-balanced multiplier (DBM) and parasitic elements around the fed patch. The DBM-integrated CP antenna theoretically provides wideband 90° phase difference between two orthogonal modes. The parasitic elements improve the amplitude imbalance of the two modes as the parasitic elements are designed to have a slightly different resonance frequency from the fed patch. The 3-dB axial-ratio bandwidth of the 5-GHz band prototype antenna is around 10.9% for both polarization senses.

keywords: *Parasitic element, wideband circular polarization, polarization switchable, DBM.*

1. Introduction

Wireless communication systems employing circularly polarized (CP) antennas have many advantages over linear polarization systems [1]. One of the advantages is mitigating the multipath fading. Reconfigurable CP antennas which switch the polarization between the right-hand circular polarization (RHCP) and left-hand circular polarization (LHCP) maximize the polarization efficiency. To realize the polarization switchable CP antennas, many studies have been conducted using microstrip antennas, which have a simple structure and are easy to be fabricated. In general, there are two ways to achieve the polarization switchable microstrip CP antenna: using a reconfigurable radiation element [2]–[8] and using a reconfigurable feeding network [9]–[11]. The former antennas have simple configuration, but the bandwidth is narrow. On the other hand, the latter has good CP characteristics over a relatively wide frequency band. But it requires additional circuit elements such as a 3-dB hybrid, which occupies a large area on the antenna. Therefore, if we have a simple and wideband reconfigurable CP microstrip antenna, the degree of freedom in designing wireless systems can be increased. It also contributes to improve the system performance.

To achieve such an antenna, we have reported a CP switchable microstrip antenna based on a new CP excitation principle [12]. The antenna provides a wideband circular polarization by effectively utilizing a double-balanced multiplier (DBM) consisting of four diodes. Due to the function of the DBM, the phase difference of the orthogonal resonance modes can be set to around 90 degrees in a wide frequency band. As a result, wideband CP operation can be achieved despite the single feed antenna.

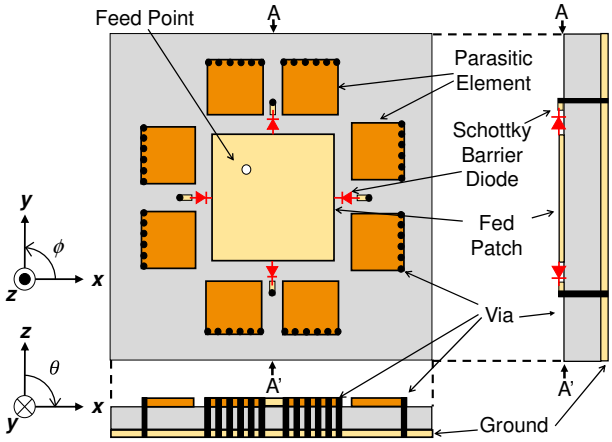

Fig. 1 Antenna configuration.

In this paper, parasitic elements are loaded to a DBM-integrated CP switchable microstrip antenna. The proposed antenna is a single-feed antenna and has wideband CP characteristics. Furthermore, it can switch the RHCP and LHCP with a simple configuration. The proposed antenna contributes to realize high-speed and large-capacity wireless communication systems in the next generation.

2. Configuration and Structure

Fig. 1 shows the configuration of the proposed CP switchable antenna. Anode or cathode of four Schottky barrier diodes is connected at the center of each side of the square fed patch. The other side of the diode is grounded through a via. These connections form a star-shaped DBM. Eight parasitic elements are capacitively coupled to the fed patch, and the outer side of each parasitic element is grounded. The length of the parasitic element is less than half of the fed patch.

[†]The authors are with Department of Electrical and Electronic Engineering, Saga University, 840–8502, Japan.
a) E-mail: kayashima08@ceng.ec.saga-u.ac.jp
b) E-mail: nisiyama@ceng.ec.saga-u.ac.jp
c) E-mail: toyoda@cc.saga-u.ac.jp

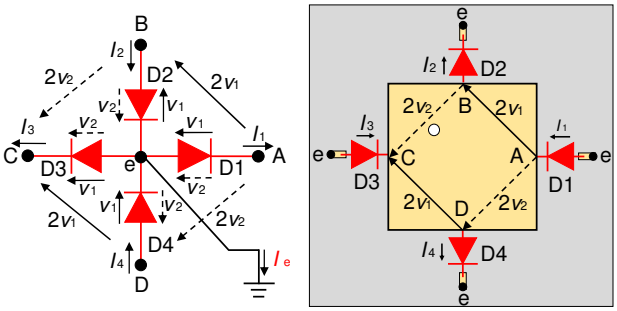

(a) Equivalent circuit (b) DBM-integrated antenna

Fig. 2 Basic behavior of the star-shaped DBM.

3. Operating Principle

3.1 Star-shaped DBM

CP requires two orthogonal modes with the phase difference of $\pm 90°$ and the same amplitude. To achieve a wideband operation, these conditions have to be maintained in a wide frequency band.

Fig. 2 shows the equivalent circuit of the star-shaped DBM and its corresponding layout of the DBM-integrated antenna. As shown in Fig. 2(a), the anode of the diode D1 and D3, and the cathode of D2 and D4 are connected at point e. When the amplitudes of two orthogonal modes are v_1 and v_2, the voltage differences among A, B, C and D are $2v_1$ and $2v_2$ as shown in Fig. 2(b). Therefore, the voltages applied to the diodes become v_1 and v_2.

Assuming v_1 and v_2 as follows:

$$v_1 = V_1 \cos(\omega t + \theta_1) \quad (1)$$

$$v_2 = V_2 \cos(\omega t + \theta_2), \quad (2)$$

the current flow to the point e can be expressed in the following expression.

$$I_e = -I_1 + I_2 - I_3 + I_4$$
$$= 8AV_1V_2[\cos(2\omega t + \theta_1 + \theta_2) - \cos(\theta_1 - \theta_2)] \quad (3)$$

where A is an amplitude coefficient. Therefore, the DC component of (3) is expressed in the following equation.

$$I_{ed} = 8AV_1V_2 \cos(\theta_1 - \theta_2) \quad (4)$$

When the DC voltage at e is set to 0 V by applying a bias voltage, the DC current I_{ed} has to be 0. Then,

$$\theta_1 - \theta_2 = \pm\frac{\pi}{2}. \quad (5)$$

Therefore, the two orthogonal modes are coupled with a phase difference of $\pm 90°$ [13]. As the relation in (5) does not depend on the frequency, wideband CP operation can be achieved. Furthermore, the CP sense can be switched by the polarity of the bias voltage.

3.2 Parasitic Elements

Fig. 3 shows a comparison of the simulated axial ratio (AR) and amplitude difference of the radiated electric fields E_x and E_y of the DBM-integrated CP switchable microstrip antenna with and without parasitic elements. As shown in

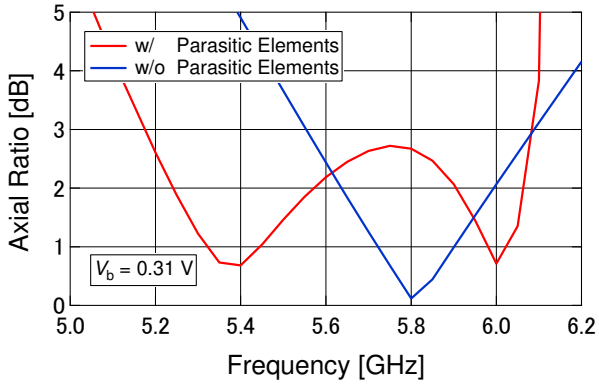

(a) Axial ratio

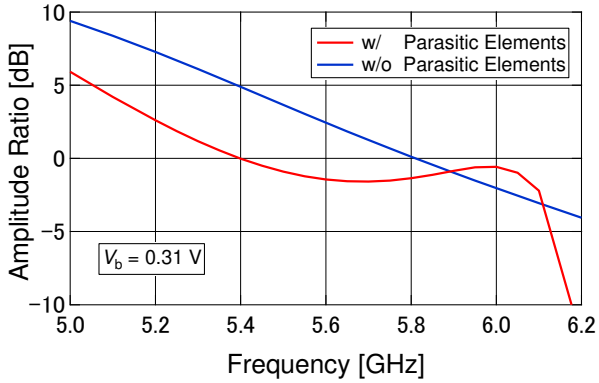

(b) Amplitude ratio E_x/E_y

Fig. 3 Comparison of the simulated results w/ and w/o parasitic elements.

Fig. 3(a), the AR less than 1 dB are obtained regardless of the parasitic elements. In the case of the antenna without parasitic elements, the 3-dB AR bandwidth is 8.6% from 5.55 to 6.05 GHz. The bandwidth is much wider than those of ordinary single-feed CP antennas. However, the AR graph has a valley even though the phase difference is maintained in a wide frequency band. The reason is that the amplitude difference, which is another factor of the axial ratio, decreases monotonically as shown in Fig. 3(b).

On the other hand, in the case of the parasitic-loaded antenna, the 3-dB AR bandwidth increases to about 15.1% from 5.2 to 6.05 GHz. As the parasitic elements are designed to have a slightly higher resonance frequency than that of the fed patch, the orthogonal modes of the proposed antenna respectively have two resonance frequencies. Furthermore, the amplitudes of the orthogonal modes become the same (i.e., 0 dB) around the frequencies as shown in Fig. 3(b). As each patch size is adjusted so that these frequencies fall within the range of 90° phase difference created by the DBM, the AR has two valleys less than 1 dB around the two frequencies, 5.4 and 6.0 GHz. The simulation and design utilized a combination of electromagnetic simulation and harmonic-balance circuit simulation in Advanced Design System (ADS ver. 2021, Keysight Technologies) [14].

4. Experimental Results

Fig. 4 shows the dimensions and a photograph of the

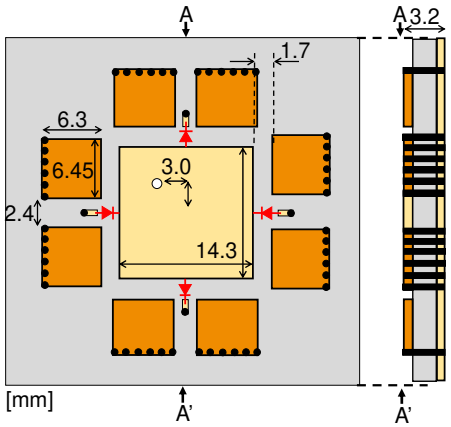

(a) Antenna dimensions

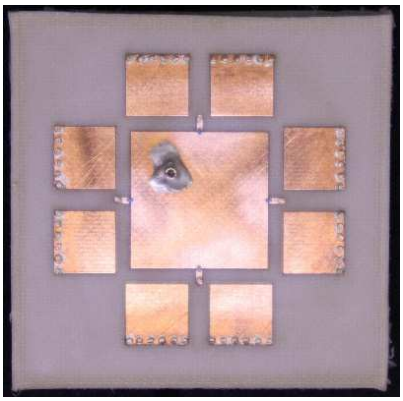

(b) Photograph (40 × 40 mm)

Fig. 4 Designed and fabricated 5-GHz antenna.

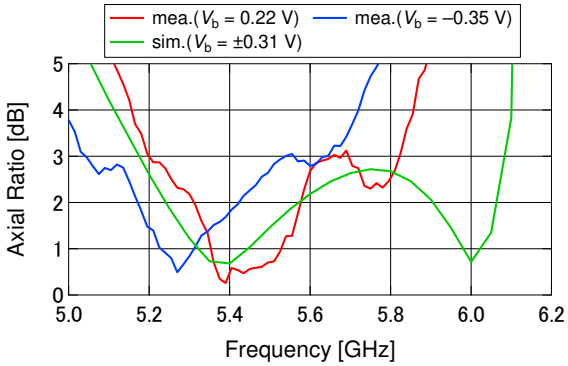

Fig. 5 Measured and simulated axial ratio of the proposed antenna.

designed prototype CP antenna. The fed patch and the ground plane are 14.3-mm and 40.0-mm square, respectively. The size of the parasitic elements is 6.3×6.45 mm. The spacing between the parasitic elements is 2.4 mm, and the gap between the fed patch and each parasitic element is 1.7 mm. These elements are etched on a polytetrafluoroethylene (PTFE) substrate ($\varepsilon_r = 2.15$, thickness = 3.2mm). The Schottky barrier diodes are SMS7630-061 (SKYWORKS). A coaxial connector is mounted on the back side of the antenna, and the bias voltage is superimposed on the RF signal using a bias tee. An Anritsu MS46322A/B network analyzer is used for the measurements.

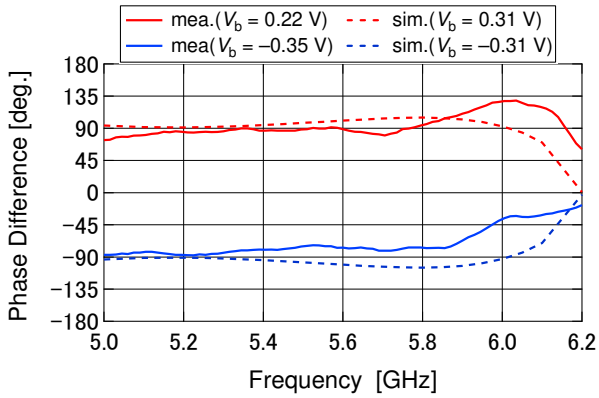

(a) Phase difference between E_x and E_y

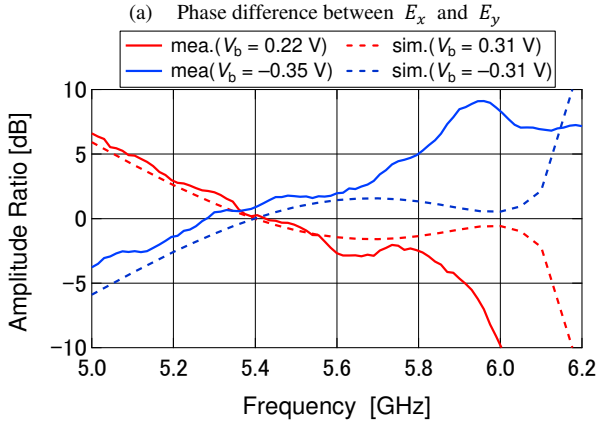

(b) Amplitude ratio E_x/E_y

Fig. 6 Phase and amplitude imbalance of two orthogonal modes.

Fig. 5 shows the measured and simulated AR of the proposed antenna. The bias voltage V_b is set to the voltage where the 3-dB AR bandwidth becomes widest, i.e., $V_b = \pm 0.31$ V in the simulation and $V_b = +0.22/-0.35$ V in the measurement. Good results of the minimum AR less than 1 dB are obtained in both simulation and measurement. In the measurement, the 3-dB AR bandwidth is approximately 10.9% from 5.21 to 5.81 GHz and 10.9% from 5.05 to 5.63 GHz for positive and negative bias voltage, respectively. Wideband performance similar to the simulated result is obtained.

Fig. 6 shows the measured and simulated phase and amplitude imbalances of the electric fields E_x and E_y. As shown in Fig. 6(a), the phase difference of $\pm 90°$ is obtained over a wide frequency range for both positive and negative bias conditions. The bandwidth with a phase difference of $90° \pm 20°$ is about 1 GHz for both simulation and measurement. It is confirmed that the DBM provides wideband $90°$ phase difference and the phase relation can be switched by the bias voltage.

On the other hand, the amplitude of E_x and E_y are equal around 5.4 GHz in the simulation and measurement as shown in Fig. 6(b) when a positive bias is applied. Furthermore, the amplitude imbalance becomes flat from 5.4 to 6.0 GHz. Similar results are obtained for the negative bias, but the frequency where the amplitude ratio equals 0 dB is 5.3 GHz instead of 5.4 GHz for the measurement. The amplitude imbalance is less than 5 dB regardless of the bias

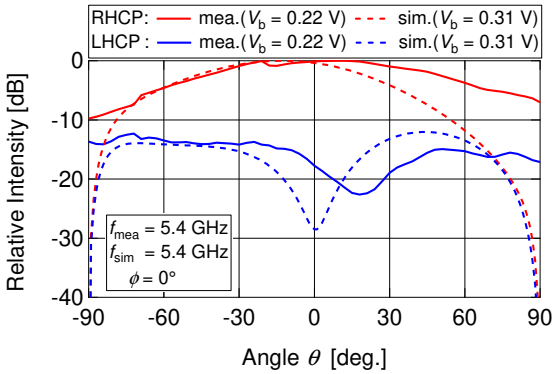

(a) Positive bias

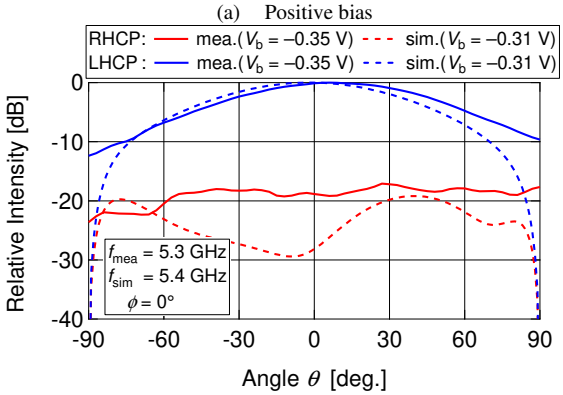

(b) Negative bias

Fig. 7 Measured and simulated radiation pattern.

polarity in a wide frequency range.

Fig. 7 shows the measured and simulated radiation patterns of the proposed antenna. Like ordinary microstrip antennas, the beam direction is the broadside direction ($\theta = 0°$). The polarization senses of the positive and negative bias conditions are RHCP and LHCP, respectively. The polarization switching is achieved. The maximum realized gains are 2.10 dBi and 2.68 dBi at $\theta = -6°$ for RHCP and LHCP, respectively. The reasons of the low realized gain are impedance mismatching and loss of the diodes.

5. Conclusion

A new wideband DBM-integrated CP switchable microstrip antenna with parasitic elements has been proposed. The wideband CP characteristics are obtained in both CP senses by effectively using a DBM-integrated CP antenna and parasitic elements. The measured 3-dB AR bandwidth is around 10.9% for both polarization senses. The proposed antenna increases the design flexibility of the wireless communication systems and contributes to the development of next generation wireless communication systems.

References

[1] A. Kajiwara, "Line-of-sight indoor radio communication using circular polarized waves," *IEEE Trans. Veh. Technol.*, vol. 44, no. 3, pp. 487–493, Aug. 1995.

[2] F. Yang and Y. Rahmat-Samii, "A reconfigurable patch antenna using switchable slots for circular polarization diversity," *IEEE Microw. Wireless Compon. Lett.*, vol. 12, no. 3, pp. 96–98, Mar. 2002.

[3] M. K. Fries, M. Grani, and R. Vahldieck, "A reconfigurable slot antenna with switchable polarization," *IEEE Microw. Wireless Compon. Lett.*, vol. 13, no. 11, pp. 490–492, Nov. 2003.

[4] R.-H. Chen and J.-S. Row, "Single-fed microstrip patch antenna with switchable polarization," *IEEE Trans. Antennas Propag.*, vol. 56, no 4, pp. 922–926, Apr. 2008.

[5] T. Song, Y. Lee, D. Ga, and J. Choi, "A polarization reconfigurable microstrip patch antenna using PIN diodes," *Proc. 2012 Asia-Pacific Microw. Conf. (APMC)*, Kaohsiung, Taiwan, 3B4-08, pp. 616–618, Dec. 2012.

[6] N. H. Noordin, W. Zhou, A. O. El-Rayis, N. Haridas, A. T. Erdogan, and T. Arslan, "Single-feed polarization reconfigurable patch antenna," *2012 IEEE Int. Symp. Antennas Propag. and USNC/URSI National Radio Sci. Mtg. (APSURSI2012) Dig.*, Chicago, IL, USA, Jul. 2012.

[7] B. Kim, B. Pan, S. Nikolaou, Y.-S. Kim, J. Papapolymerou, and M. M. Tentzeris, "A novel single-feed circular microstrip antenna with reconfigurable polarization capability," *IEEE Trans. Antennas Propag.*, vol. 56, no. 3, pp. 630–638, Mar. 2008.

[8] Y.-F. Wu, C.-H. Wu, D.-Y. Lai, and F.-C. Chen, "A reconfigurable quadri-polarization diversity aperture-coupled patch antenna," *IEEE Trans. Antennas Propag.*, vol. 55, no. 3, pp. 1009–1012, Mar. 2007.

[9] L. Bian, Y.-X. Guo, L. C. Ong, and X.-Q. Shi, "Wideband circularly polarized patch antenna," *IEEE Trans. Antennas Propag.*, vol. 54, no. 9, pp. 2682–2686, Sep. 2006.

[10] S. Maddio, A. Cidronali, I. Magrini, and G. Manes, "A design method for single-feed wideband microstrip patch antenna for switchable circular polarization," *Proc. 37th European Microwave Conf. (EuMW2007)*, Munich, Germany, pp. 262–265, Oct. 2007.

[11] K. Boonying, C. Phongcharoenpanich, and S. Kosulvit, "Polarization reconfigurable suspended antenna using RF switches and P-I-N diodes," *Proc. 4th Joint Int. Conf. Info. Commun. Technol., Electron. Electrical Eng. (JICTEE),* Chiang Rai, Thailand, pp. 1–4, Mar. 2014.

[12] E. Nishiyama, A. Matsuo, and I. Toyoda, "Double balanced multiplier integrated circular polarization switchable microstrip antenna," *2015 IEEE Int. Symp. Antennas Propag and SNC/URSI National Radio Sci. Mtg. (AP-S/URSI2015) Dig.*, Vancouver, BC, Canada, pp. 2239–2240, Jul. 2015.

[13] E. Nishiyama, T. Ino, and I. Toyoda, "Experimental study of double-balanced-multiplier integrated circularly polarized microstrip antenna for Tx and Rx operation (Invited)," *Proc. 2017 IEEE Int. Symp. Radio-Frequency Integ. Tech. (RFIT2017),* Seoul, Korea, FR_2B_1, pp. 117–119, Aug. 2017.

[14] T. Kayashima, E. Nishiyama, and I. Toyoda, "Novel simulation approach to microstrip antenna integrated with nonlinear circuit," *Proc. 2020 Int. Symp. Antennas Propag. (ISAP2020)*, Osaka, Japan (Virtual), pp. 187–188, Jan. 2021.